Dynamics of electron transfer at polar molecule-metal interfaces: The role of thermally activated tunnelling

Short Title: Dynamics of electron transfer at polar molecule-metal interfaces

J Stähler, M Meyer, X Y Zhu[1], U Bovensiepen, and M Wolf [2]
Freie Universität Berlin, Fachbereich Physik, Arnimallee 14, 14195 Berlin, Germany
E-mail: wolf@physik.fu-berlin.de

Abstract. Heterogeneous electron transfer across interfaces is frequently discussed on the basis of Marcus Theory taking into account rearrangements of the solvent along a nuclear coordinate *q*. The electron transfer process itself occurs via tunnelling through a barrier normal to the interface. The key point is not whether tunnelling occurs, but whether thermally activated solvent fluctuations initiate the tunnelling. Here, we discuss the role of thermally activated tunnelling in heterogeneous electron transfer versus direct electron transport due to strong electronic coupling to a metal substrate. As a model system we investigate the ultrafast dynamics of electron transfer at amorphous ice-metal interfaces (4-6 bilayers D_2O/Cu(111) and Ru(001), respectively) by time-resolved two-photon photo-electron spectroscopy. We find that the electron transfer rate is *independent* of temperature within the first 500 fs after excitation, which demonstrates that for this system interfacial electron transfer occurs in the strong coupling limit and that thermally assisted tunnelling plays a negligible role.

PACS: 73.90.+f, 78.47.+p, 79.60.Dp, 31.70.Hq

[1] University of Minnesota, Department of Chemistry, Mineapolis, Minnesota 55455, USA
[2] Author to whom any correspondence should be addressed.

1. Introduction

Electron transfer (ET) from a molecular donor to an acceptor state is one of the simplest conceivable reactions, as chemical bonds are neither formed nor broken. Such charge transfer reactions are of vital importance to a variety of processes in physics, chemistry and biology. For example, homogeneous ET is the primary step in photosynthesis [1,2] and various chemical reactions [3,4]. Heterogeneous ET at molecule-solid interfaces, on the other hand, plays an important role in technologically highly relevant fields. Examples are dye-sensitized solar (Grätzel) cells where light is converted into electrical energy by photo-excitation of adsorbed dye molecules and subsequent charge injection into the conduction band of a semiconductor substrate [5]. In addition, charge injection from a conducting electrode to a molecular system is of key relevance for the development of organic optoelectronic and nanoscale molecular devices [6,7]. Furthermore, in the field of photochemistry at metal surfaces, transfer of photoexcited substrate electrons into unoccupied orbitals of adsorbed molecules provides a mechanism to induce chemical reactions by energy transfer to vibrational motion of the adsorbate. [8,9]

Different theoretical descriptions of charge transfer processes have been developed in the past [10]. Heterogeneous ET has been considered to occur along a real space electron transfer coordinate, where tunnelling of the electron is mediated by wave function overlap between donor and acceptor states. This picture has been frequently applied to describe the population decay of image potential states at metal surfaces [11] or the excitation process in surface photochemistry [12]. Depending on the degree of coupling between the electronic levels, a tunnelling barrier is assumed at the interface that determines the electron transfer rate, whereby solvent fluctuations are assumed to play a negligible role [12]. An apparently different concept for charge transfer phenomena is the Marcus Theory [13,14,15], which was originally developed to describe *homogeneous* ET (e.g. in solution) between two molecular levels. In this theory, charge transfer is rate-limited by nuclear motion of solvent molecules which arrange differently depending on the charge distribution of the solute (e.g. in donor-bridge-acceptor systems). The Marcus Approach has also been extended to the heterogeneous ET problem and applied to charge transfer phenomena at molecule-semiconductor interfaces (e.g. dye-sensitized solar cells) [10, 16] and ET at organic-metal interfaces [17].

However, it should be noted that these seemingly different concepts for ET (Marcus Theory versus tunnelling picture) are indeed complementary, as in general charge transfer will involve both nuclear rearrangement *and* tunnelling along the real space transfer coordinate. For a detailed understanding, identification of the actual *rate-determining step* is required*:* Coupling between the electronic levels or solvent rearrangement. Thus, both

pictures of charge transfer should be considered as a certain limit of a unifying concept, which involves both the electron and the nuclear (solvent) coordinates. This has been explained nicely by Truhlar and co-workers, who derived a theory for charge (proton) transfer taking into account both real space and solvent coordinates [18]. Truhlar's concept uses a two dimensional potential energy landscape that reflects the system's evolution from a donor to an acceptor state as a function of solvent *and* solute coordinate, respectively. The main idea is to treat the solvent and solute coordinate "on a nearly equal footing" and to understand the crossover between solvent-controlled and solvent-independent dynamics.

The corresponding 2D potential for *heterogeneous* ET from a solvated state (e.g. in a polar adsorbate layer [19,20,21] to a metal electrode has to take into account the delocalized nature of electronic states and the existence of a continuum of accepting states in the metal substrate. Figure 1 depicts a schematic contour plot of such a potential energy landscape of the solvated electron (donor state) and the lowest unoccupied (acceptor) states of the metal as a function of lattice distortion q (vertical axis) and electron transfer coordinate z (bottom axis). The grey shaded area corresponds to the metal and the white background to the adsorbate layers. As discussed in more detail below (see section 2), cuts through the 2D potential surface along either the electron transfer coordinate z or the solvent coordinate q result in the electron potential energy along z for a fixed solvent distortion (panel b) [22] or in the Marcus Parabolas for donor (V_D) and acceptor (V_A) states (panel c), respectively. The horizontal and vertical dashed lines indicate the corresponding cuts. However, it should be noted that this extension of Truhlar's concept to a 2D potential for heterogeneous ET is just schematic in order to illustrate the connection between the solvent motions and the electron tunnelling.

In this manuscript, we discuss the role of thermally activated tunnelling in heterogeneous ET at a metal surface. The key question is not whether tunnelling occurs, but whether thermally activated solvent fluctuations lead to instantaneous reduction of the tunnelling barrier and thus mediate the tunnelling rate. On the other hand, for sufficiently strong wave function overlap of the excess electron with unoccupied metals states, direct transport without changes of the solvent configuration will dominate. In this work, we study the ultrafast electron solvation dynamics at amorphous ice-metal interfaces (several bilayer (BL) of D_2O adsorbed on Cu(111) and Ru(001)) using femtosecond time-resolved two-photon photoemission (2PPE) spectroscopy [23,24]. Depending on the degree of coupling between the solvated excess electron in ice and the electronic states in the metal, different limits will be applicable for the description of the ET process. We discuss which coordinate, z or q, is most relevant for the charge transfer process at amorphous ice-metal interfaces. To

do so, understanding of the influence of temperature on the ET rate is necessary as a thermally activated solvent rearrangement may facilitate the transfer process.

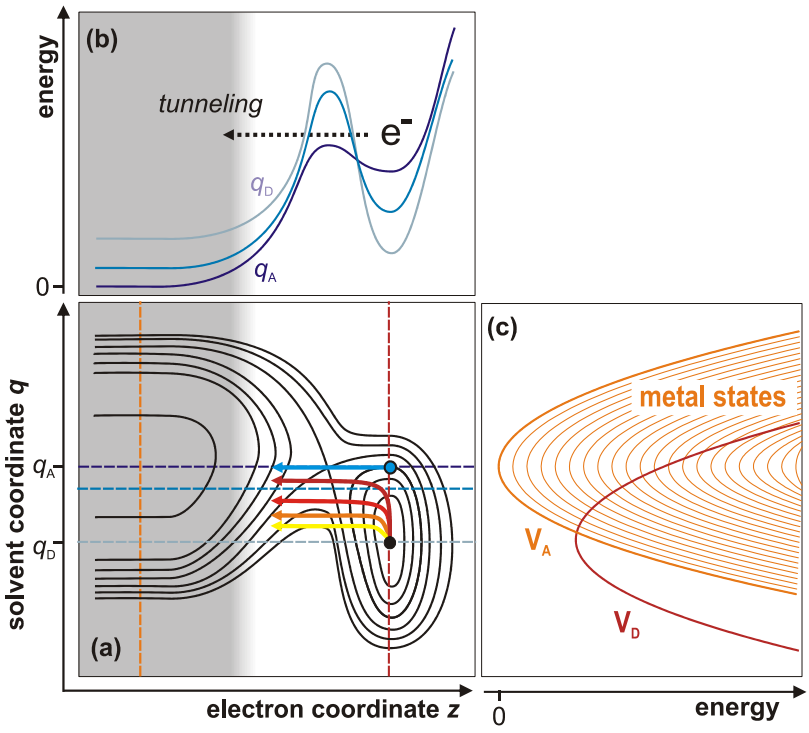

Figure 1. Two-dimensional model for ET at a metal surface: (a) 2D potential energy surface of the electron-metal/solvent system for the donating polar adsorbate and the energetically lowest unoccupied (accepting) metal substrate state along the real space coordinate z and the solvent coordinate q. Arrows illustrate direct electron transport due to strong electronic coupling (blue) and due to thermally assisted tunnelling (yellow to red, see section 2) (b) Horizontal cuts give the potential along the electron coordinate for a fixed lattice distortion. c) Marcus parabolas of the solvated electron and the lowest unoccupied metal state (thick curves). The continuum of unoccupied acceptor states above V_A is denoted by the thinner orange lines.

In section 2, the temperature dependence of the classical Marcus Approach will be discussed. As this theory of non-adiabatic ET is based on the assumption that the solvated electron is thermally equilibrated with its surrounding, it hast to be adjusted to describe the temperature dependence of a just photoinjected excess electron. Subsequently, charge transfer in the strong coupling limit will be discussed. After a brief description of 2PPE spectroscopy (section 3), temperature-dependent measurements of the electron transfer dynamics at amorphous ice-metal interfaces will be presented in section 4. The results allow for the determination of the rate-limiting step for charge transfer, i.e. solvent fluctuation or coupling strength. We find for amorphous D_2O metal interfaces that the dynamics of

electron transfer directly after photoinjection is *not* thermally activated, which shows that ET at the investigated ice-metal interfaces occurs in the strong coupling limit.

2. Marcus theory for heterogeneous ET and the role of thermal activation

In the following, we discuss the role of thermally activated tunnelling versus electron transport by direct electronic coupling to a metal substrate using Marcus Theory. Originally, Marcus developed his charge transfer theory for *homogeneous* transfer within a solvent, i.e. for the ET from one distinct molecular state to another. [13,14,15] The main challenge was to find a simple description for this multidimensional problem of donor, acceptor, and the abundance of solvent molecules. In his classical theory, Marcus assumed that the motions of the solvent molecules occur within linear response limits, i.e. the displacements are so small that the assumption of a harmonic intermolecular potential is applicable. [25] However, the infinite number of possible solvent configurations would lead to an enormously complex multidimensional potential energy surface. The black parabolas in figure 2a are slices through this energy landscape along a generalized solvent coordinate, assuming a fixed distance of donor and acceptor.

These potentials, V_D and V_A for donor and acceptor, respectively, are plotted as a function of the collective solvent coordinate q. This coordinate describes changes in the molecular configuration of the solvent. The potential minima at q_D and q_A correspond to the fully equilibrated species of donor and acceptor. At the so-called adiabatic crossing point q_t, fluctuations of the solvent bring these two levels in resonance; this transition state region is often termed the adiabatic crossing point. Depending on the coupling strength V_{DA} between the two states, an avoided crossing of the potential occurs (see further below). In this *strong coupling limit* charge transfer occurs adiabatically: If the system passes the "intersection" by fluctuation, it will remain at the lowest potential. If there were *no* coupling between the levels, charge transfer would not occur at all. Considering very *weak coupling* between donor and acceptor, fluctuations across q_t would make the system traverse to the upper potential surface and back; [26] in this case ET occurs with the probability

$$k_{\text{homo}} = \frac{2\pi}{\hbar} \cdot \langle V_{DA} \rangle^2 \cdot FC, \qquad (1)$$

where V_{DA} is the coupling matrix element between donor and acceptor level and FC is a thermally averaged Franck-Condon factor that describes the influence of temperature on the charge transfer rate by a Boltzmann distribution of the vibronic levels in the harmonic (parabolic) potential. The ET probability is thereby determined by the nuclear potential barrier ΔE, which is the energy difference between the intersection at q_t and the donor potential minimum at q_D. It depends on the reorganization energy λ and the free energy of the reaction ΔG_0.

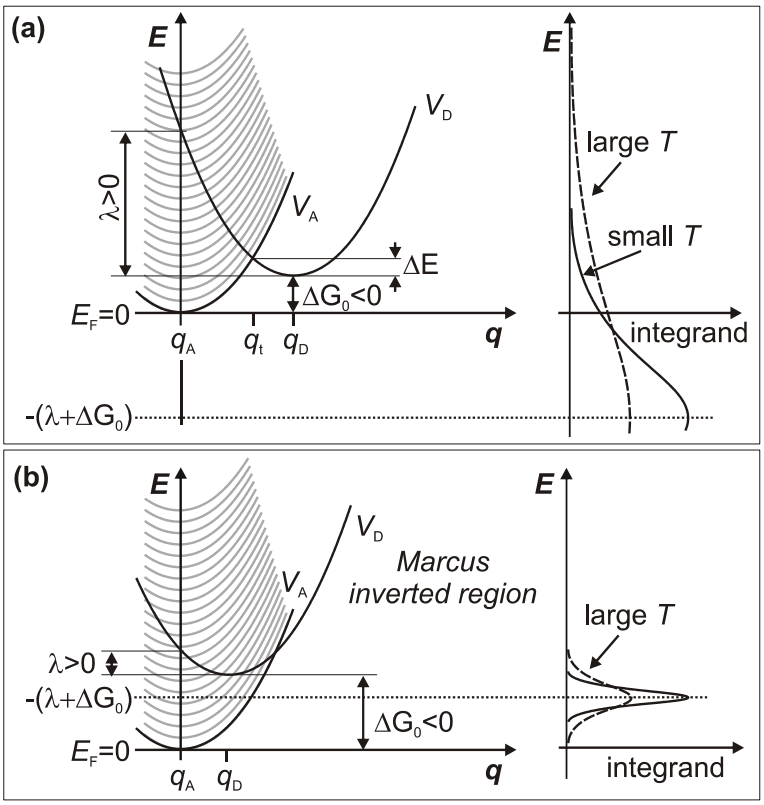

Figure 2. Marcus Curves for heterogeneous ET from a molecular donor state V_D to a continuum of accepting substrate states (grey curves). (a) For $\lambda + \Delta G_0 > 0$ the charge transfer rate can be temperature-dependent, as the Gaussian distribution (right) is cut by the Fermi Function according to equation (2). (b) In the inverted region, i.e. $\lambda + \Delta G_0 < 0$, ET is temperature-independent for sufficiently large $|\Delta G_0|$, as the Fermi Function in equation (2) does not cut the Gaussian distribution considerably (right).

Extension of this model to the *heterogeneous* problem, i.e. the transfer from a distinct molecular state to a metal (electrode) offering a continuum of unoccupied states above the Fermi Level E_F, requires a continuum of accepting states as illustrated by the grey curves in figure 2a. [7,10] The energetically lowest level corresponds to the lowest unoccupied states of the metal close to E_F, here denoted as V_A. The transfer rate from the donor state V_D to V_A exactly follows equation (1). However, transfer to the energetically higher lying states in the metal also contributes to the transfer rate. Thus, consideration of the varying energy difference between the respective parabola minima is required. Integration of the resulting rate constants weighted by the Fermi-Dirac distribution $f(E)$ around E_F and the metal's DOS $\rho(E)$ leads to the total rate of heterogeneous ET [20]:

$$k_{\text{hetero}} = \int_{-\infty}^{\infty} \frac{2\pi}{\hbar} \cdot \langle V_{DA} \rangle^2 \cdot (1 - f(E)) \cdot \rho(E) \cdot \left(\frac{1}{4\pi\lambda k_B T} \right)^{\frac{1}{2}} \cdot \exp\left\{ - \frac{[E + (\lambda + \Delta G_0)]^2}{4\lambda k_B T} \right\} \mathrm{d}E \quad (2)$$

For constant coupling V_{DA} and density of states $\rho(E)$ this expression can become temperature-dependent if $(\lambda+\Delta G_0) > 0$, i.e. the minimum of V_D lies below the intersection with V_A (cf. figure 2a). ET requires thermal activation to overcome ΔE, or, in other words, the Gaussian distribution in equation (2) is cut by the Fermi Function (cf. figure 2a, right) maintaining the temperature dependence of equation (2) after integration. If $(\lambda+\Delta G_0) < 0$ the donor parabola V_D is in the inverted region (cf. figure 2b). This means that V_D is intersected by acceptor levels down to its minimum and non-activated charge transfer can occur at any $q<q_D$, regardless of the Boltzmann distribution of donor states. If the Gaussian's width $(4\lambda k_B T)^{1/2}$ is sufficiently small ($|\Delta G_0|$ sufficiently large), the distribution is not considerably cut by the Fermi Function (cf. figure 2b, right). This leads to a temperature *independence* of ET, as both temperature-dependent factors in equation (2) are cancelled by integration.

Note, that the above described approach of weak electronic coupling is based on the assumption of a thermally equilibrated system in the donor state [10]. This means that the process of electron solvation (i.e. equilibration with the solvent) has to occur on a much faster timescale than the electron transfer. Such a Boltzmann distribution of molecular modes is not necessarily reached for excited ("hot") electrons in molecular adlayers on metal surfaces, as the transfer occurs here on fs-timescales. For these systems, electron transfer and solvation compete with each other [24] and a thermally equilibrated solvated electron distribution around the potential minimum cannot be assumed. Figure 3a illustrates ET of a nascent excess electron en route to localization due to solvation, but has not reached the potential minimum of V_D. The energy barrier ΔE^*_{exc} for charge transfer to the exemplary metal state V_A^* for the non-equilibrium, "hot" electron is smaller than that for the equilibrated electron (ΔE^*_{equi}) by $E_S + \Delta G_0$. This reduction adds an additional exponential factor in the transfer rate integral in equation (2):

$$k(E_S) \propto \int \frac{2\pi}{\hbar} \cdot \langle V_{DA} \rangle^2 \cdot (1 - f(E)) \cdot \rho(E) \cdot \left(\frac{1}{T}\right)^{\frac{1}{2}}$$

$$\times \exp\left(\frac{E_S + \Delta G_0}{k_B T}\right) \exp\left\{-\frac{\left[E + (\lambda + \Delta G_0)\right]^2}{4\lambda k_B T}\right\} \qquad (3)$$

The term $E_S+\Delta G_0$ is always positive and becomes zero when the solvated electron is fully equilibrated. It introduces a temperature dependence of the transfer rate, which is *not* cancelled out in contrast to the case of the equilibrium description in the Marcus inverted region (figure 2b). In conclusion, in this picture, where constant V_{DA} and $\rho(E)$ are assumed, charge transfer is *always* temperature-dependent as long as the system has not reached the V_D minimum ($E_S + \Delta G^0 > 0$).

In fact, the assumption of energy-independent V_{DA} and ρ is questionable, since a solvated electron dynamically *changes* its degree of confinement, as shown in a previous publication [19]. Thus, the assumption of a constant coupling matrix element V_{DA} certainly does not hold true. Instead, the coupling decreases significantly upon solvation (see Ref. [24]). Equation (2) becomes independent of temperature only if the integrand remains a Gaussian with an energy-independent amplitude proportional to $T^{-1/2}$. Thus, *any* energy dependence of the pre-factors in equation (2) that varies the Gaussian distribution results in a temperature dependence of the transfer rate. A change of $V_{DA}(E)$ due to dynamic solvation can therefore cause a temperature dependence of the system, even if it is in the Marcus inverted region and in thermal equilibrium.

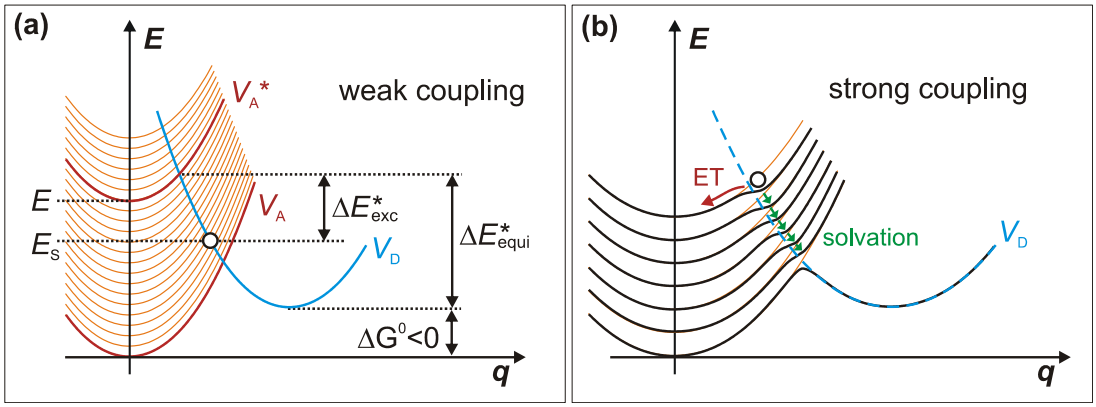

Figure 3. Heterogeneous ET of just photoinjected, excited electrons. (a) Weak coupling limit: The nuclear barrier ΔE^*_{hot} is reduced by $E_S + \Delta G_0$ introducing an additional temperature dependence of the transfer rate. (b) Strong coupling limit: Schematic illustration of adiabatic, barrier-free electron transfer due to avoided crossing of electronic levels (red arrow), which competes with solvation (green arrows).

Having shown, that heterogeneous ET in the weak coupling limit is governed by a temperature dependence of the charge transfer rate, we now turn to a discussion of heterogeneous ET in the strong coupling limit. Here, the donor and acceptor potentials split in the crossing point region so that ET proceeds adiabatically (cf. figure 3b) [10]. The degree of level splitting is determined by the coupling strength. Thus, the nuclear barrier can vanish as schematically sketched in figure 3b. Accordingly, solvent rearrangement is not the rate-limiting step in this regime of charge transfer, as the system can proceed barrierfree downwards the potential energy surface. At the same time, solvation (green arrows) competes with the ET: Progression to larger q occurs with a certain probability. However, the transfer is solely determined by the coupling matrix element V_{DA} and mediated by

electron transport due to strong wave function overlap with metal states. In this regime, the interfacial electron transfer is temperature-independent.

The arrows in figure 1a indicate schematically the two regimes of interfacial ET discussed above: In the strong coupling limit (blue top arrow), electron transport occurs mainly along the electron coordinate x. The strong wave function overlap with metal states is considerably more probable than ET due to thermal activation: The coupling strength (rather than nuclear rearrangement) rate-limit the charge transfer. In the weak coupling limit (yellow to red arrows), the transfer matrix element is sufficiently small to enable thermally activated rearrangement of the solvent molecules (change of solvent coordinate q) enhancing the transfer rate: Fluctuations of the solvent to smaller q (closer to q_A) become more probable with increasing temperature. Thermal activation becomes the rate-limiting step for ET. However, it is difficult to draw a distinct line between the strong and the weak coupling limit for electron solvation at polar adsorbate-metal interfaces, as the wave function constriction and therefore the coupling of the excess electrons changes upon solvation. We consider strong and weak coupling as limiting cases of a unifying concept of interfacial ET. The present article therefore uses the term *strongly coupled* for electron transfer dominated by the electronic coupling of the solvated electron to the metal states and *not* affected by temperature variations. The weak coupling limit is reached when thermally assisted tunnelling, i.e. solvent rearrangement along q, determines the transfer rate.

3. Experimental: Time-resolved 2PPE spectroscopy

Time-resolved two-photon photoemission (2PPE) spectroscopy provides a valuable tool to investigate ultrafast electron dynamics at surfaces and interfaces [27,28]. In the past decade, surface and image potential states have been used as model systems for 2PPE and theoretical studies, leading to a profound understanding of electronic scattering and relaxation processes at bare metal surfaces [11]. Furthermore, 2PPE spectroscopy has been used to gain insights into electron transfer processes at rare gas-metal interfaces [29,30,31] and solvation dynamics of photoinjected electron in polar adsorbate layers [21,32,33].

In 2PPE, electrons are excited by an ultrashort laser pulse (with photon energy $h\nu_1$) from below the Fermi Level E_F to bound intermediate states below the vacuum level E_{vac}, where they may subsequently relax to energetically lower lying states. These electrons are excited by a second, time-delayed laser pulse ($h\nu_2$) to the continuum of final states. Figure 4a illustrates the process for photoinjection and solvation dynamics at the D_2O/Cu(111) interface. The dynamics can be separated into three steps [23]. (1) Photoexcitation from the metal substrate into the conduction band of the ice layer (note that

$h\nu_1$ is much smaller than the band gap of ice and cannot excite electrons inside the D_2O adlayer). (2) Localization in pre-existing solvation sites and energetic stabilization by molecular reorganization of the polar environment. (3) Decay of the solvated electron population by ET back to unoccupied states of the metal substrate. As shown previously, these dynamics can be viewed as a competition between charge transfer and solvation [24].

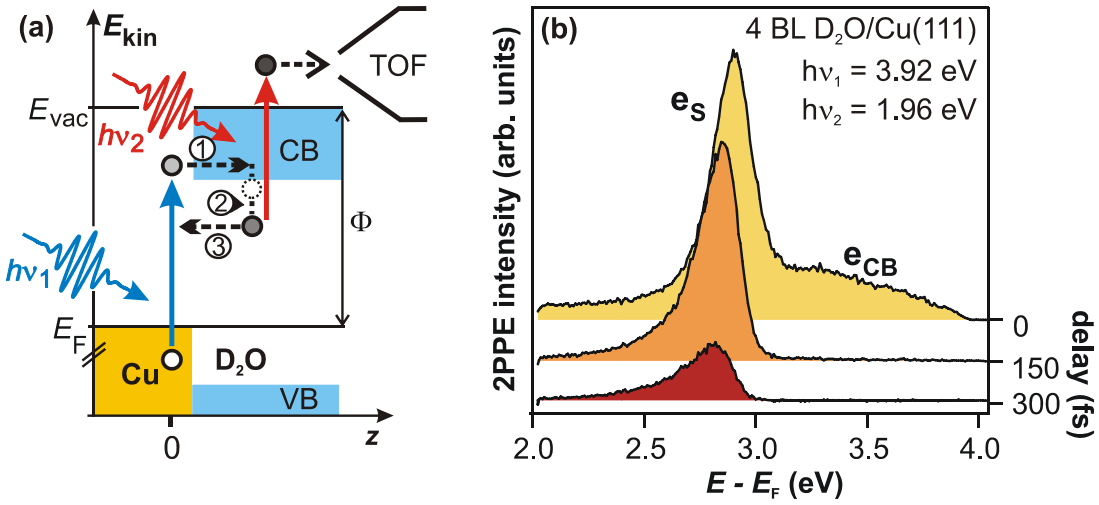

Figure 4. (a) 2PPE spectroscopy and electron localization and solvation dynamics at the ice metal interface. (b) Exemplary 2PPE spectra of 4 BL amorphous D_2O/Cu(111) for different time delays.

Our experimental setup combines an ultrahigh vacuum (UHV) chamber (base pressure < 10^{-10} mbar) for sample preparation and photoelectron spectroscopy with a tuneable femtosecond laser system (for details see Ref. 34). The photoelectron kinetic energy E_{kin} is analyzed by a time-of-flight (TOF) spectrometer and the intermediate state energy is determined as $E\text{-}E_F = E_{kin} + \Phi - h\nu_2$, where $h\nu_2$ is the probing photon energy and Φ the sample work function [35]. Amorphous D_2O films are grown at 100 K on a Cu(111) or Ru(001) single crystal surface, cleaned by standard procedures [24]. Exemplary 2PPE spectra of 4 BL amorphous D_2O/Cu(111) are depicted in figure 4b and exhibit a pronounced peak e_S, which is attributed to solvated electrons, and a broad feature e_{CB}, which is resulting from photoinjected electrons in the ice conduction band [23]. After a rapid decay of e_{CB} within the laser pulse duration, the binding energy of the solvated electrons increases (peak shift of e_S) due to screening and stabilization of the excess charge within the ice.

4. Electron transfer and solvation dynamics at the D_2O/metal interface

In the following, we discuss the influence of temperature on the ultrafast dynamics of ET at amorphous D_2O/metal interfaces. As outlined in section 2, the temperature dependence of the ET rate offers information about the coupling strength of the solvated electron to the metal states. In the case of weak electronic coupling of a photoinjected

excess electron, the rate of ET is temperature-dependent due to the reduced nuclear barrier and varying coupling matrix elements V_{DA} (see figure 3a). In the strong coupling limit, ET occurs adiabatically and – depending on the coupling strength – the nuclear barrier vanishes (figure 3b). In this regime of charge transfer, no temperature dependence of the transfer rate is expected, as electron transport due to the large wave function overlap is much more probable than transfer mediated by thermal fluctuations of the solvent.

Temperature-dependent 2PPE measurements were performed for the D_2O/Cu(111) and D_2O/Ru(001) systems to determine the regime of electronic coupling, strong or weak, for electron transfer at ice-metal interfaces. Figure 5 depicts the temporal evolution of the 2PPE intensity of the solvated electron state e_S for D_2O layers adsorbed on the Cu(111) (blue and green) and on the Ru(001) surface (yellow and orange) for different sample temperatures. The electrons decay considerably faster on Ru(001) substrate. This effect results from the different surface electronic band structures of Ru(001) and Cu(111) as shown in a previous publication [24]. However, for both datasets, no temperature dependence of the ET rate back to the metal is observed within the first half picosecond and the investigated temperature range (25-91 K for Cu(111) and 99-119 K and Ru(001), respectively). Thus, it can be concluded that the electron transfer at the investigated ice-metal interfaces is *not* thermally activated within the first 500 fs after photoinjection despite the localized character of the solvated charge [19].

The inset of figure 5 depicts the peak shift of the solvated electron distribution at the D_2O/Cu(111) interface as a function of pump-probe time delay. The peak maximum shifts with ~200 meV/ps towards the Fermi Level, i.e. the binding energy of the solvated electrons increases. This energetic stabilization of the excess electrons results from the progression of the system along the solvation coordinate q towards the minimum of the donor potential V_D in figure 1. As apparent from the inset in figure 5, this electron solvation is temperature-independent, similar to the electron decay (transfer). It is concluded, that thermal activation of reorientations of the solvent molecules is not required for ET in these early stages of solvation. Apparently, the electric field of the excess charge is the driving force for molecular reorientations, and thermally induced fluctuations play a negligible role for stabilization.

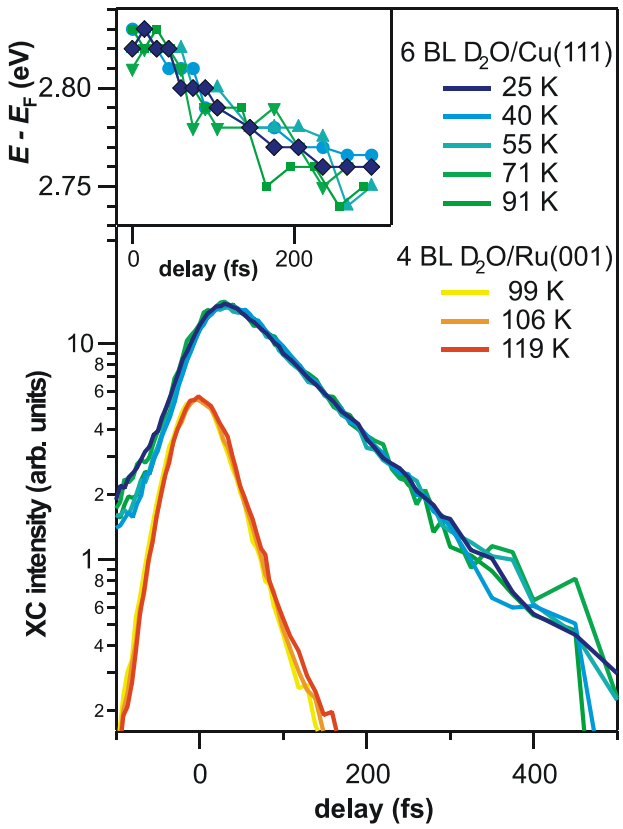

Figure 5. Temperature dependence of ET dynamics for D_2O/Cu(111) and Ru(001). Population dynamics of solvated electrons at amorphous ice-metal interfaces. The decay is independent of temperature between 25 and 119 K. Inset: Shift of the e_S maximum as a function of time delay for D_2O/Cu(111). No temperature dependence is observed.

The temperature independence of both, population decay *and* electron solvation, shows that the initial electron dynamics at amorphous ice-metal interfaces (i.e. directly after photoinjection) are mediated by strong electronic coupling: (i) Screening of the excess charge is not affected by temperature, but is driven by the electric field of the localized electron. This shows that the D_2O-electron complex has not reached the potential minimum and has not reached thermal equilibrium yet. (ii) In addition, ET back to the Cu(111) and Ru(001) substrates is not mediated by thermal fluctuations of the solvent. As shown in section 2, this means that the coupling between the solvated electron state and metal states is so strong, that direct transport (for fixed solvent configuration) is considerably more probable than thermally activated tunnelling. As heterogeneous ET in the weak coupling limit is temperature-dependent for non-equilibrated, "hot" electrons (see section 2), this result unambiguously shows that the heterogeneous ET observed here occurs in the *strong coupling limit*.

5. Summary and conclusions

The present contribution addresses the role of thermally activated tunnelling in heterogeneous electron transfer at ice metal interfaces. We show that strong and weak electronic coupling are limiting cases of a unifying picture of ET: Depending on the transfer matrix element (coupling strength of the interfacial electron to the substrate), either direct charge transport along the electron coordinate x or thermally assisted nuclear rearrangement of the solvent molecules (progression along the solvent coordinate q) become the rate-limiting step for ET. In the strong coupling limit, the significant wave function overlap of the solvated electron with unoccupied metal states leads to temperature-independent charge transfer. However, for weak electronic coupling between a nascent electron en route to solvation and the metal substrate, ET depends on temperature, as thermally activated solvent reconfiguration enhance the transfer rate. Time-resolved 2PPE experiments on amorphous multilayers of D_2O on Cu(111) and Ru(001) showed that both, electron transfer (back to the metal) and solvation are independent of temperature between 25 K and 119 K. Thus, heterogeneous electron transfer occurs in the strong coupling limit in these examples.

It should be noted, that the fast electron decay for ice/metal interfaces actually prohibits observation of ET in the weak coupling limit: If charge transfer would occur slower after photoexcitation, the solvent molecules would increasingly screen the excess charge and the system would proceed along the solvent coordinate q towards the potential minimum at q_D in figure 1. With ongoing solvation, the screening of the excess charge from the metal would increase, i.e. the coupling strength would decrease, and thermally activated tunnelling could be observed. Observation of such a transition to the weak coupling limit of charge transfer could be possible for solvent-solute complexes that exhibit faster screening from the metal substrate than for the ice-metal interfaces. If the decoupling from the metal states occurred *before* the whole solvated electron population decays, observation of solvent-driven ET should be possible. A promising candidate for such investigations is NH_3: As will be shown in a future publication [36], excess electrons in amorphous ammonia adlayers survive considerably longer than hydrated electrons in amorphous ice discussed in the present article.

Acknowledgements: We thank A. Nitzan & D. Truhlar for very stimulating and valuable discussions. XYZ gratefully acknowledges support by a Friedrich-Wilhelm-Bessel award of the Alexander-von-Humboldt Foundation. This work has been funded by the Deutsche Forschungsgemeinschaft through SPP 1093 and Sfb 450.

References

[1] Wasielewski M R 1992 *Chem. Rev.* **92** 435
[2] Morales R, Charon M-H, Kachalova G, Serre L, Medina M, Gómez-Moreno C and Frey M 2000 *EMBO Reports* **1** vol 3 p 271
[3] Roth H D 1990 *Topics in Current Chemistry: Photoinduced Electron Transfer I* ed J Mattay (Berlin: Springer) p 1
[4] Timpe H-J 1990 *Topics in Current Chemistry: Photoinduced Electron Transfer I* ed J Mattay (Berlin: Springer) p 167
[5] O'Regan B and Grätzel M 1991 *Nature* **353** 737
[6] Nitzan A and Ratner M A 2003 *Science* **300** 1384
[7] Zhu X-Y 2004 *J. Phys. Chem. B* **108** 8778
[8] Zhu X-Y 1994 *Ann. Rev. Phys. Chem.* **45** 113
[9] Frischkorn C and Wolf M 2006 *Chem. Rev.* **106** 4207
[10] Miller R J D, McLendon G L, Nozik A J, Schmickler W and Willig F 1995 *Surface Electron-Transfer Processes* (New York: VCH)
[11] Echenique P M, Berndt R, Chulkov E V, Fauster T, Goldmann A and Höfer U 2004 *Surf. Sci. Rep.* **52** 219
[12] Gadzuk J W 1995 *Surface Science* **342** 345
[13] Marcus R A 1956 *J. Chem. Phys.* **24** 966
[14] Marcus R A 1957 *J. Chem. Phys.* **26**, 867
[15] Marcus R A 1957 *J. Chem. Phys.* **26**, 872
[16] Nitzan A 2001 *Ann. Rev. Phys. Chem*. **52** 681
[17] Ge N-H, Wong C M and Harris C B 2000 *Acc. Chem. Res.* **33** 111
[18] Schenter G K, Garrett B C and Truhlar D G 2001 *J. Phys. Chem. B* **105** 9672
[19] Bovensiepen U, Gahl C and Wolf M 2004 *J. Phys. Chem. B* **107** 165
[20] Miller A D, Bezel I, Gaffney K J, Garret-Roe S, Liu S H, Szymanski P and Harris C B 2002 *Science* **297** 1163
[21] Zhao J, Li B, Onda K, Feng M, Petek H 2006 *Chem. Rev.* **106** 4402
[22] The potentials shown in panel b are not single particle potentials and therefore differ from the commonly used image potential.
[23] Gahl C, Bovensiepen U, Frischkorn C and Wolf M 2002 *Phys. Rev. Lett.* **89** 107402
[24] Stähler J, Gahl C, Bovensiepen U and Wolf M 2006 *J. Phys. Chem. B* **110** 9637
[25] Marcus R A 1964 *Ann. Rev. Phys. Chem.* **15** 155
[26] Marcus R A 1960 *Faraday Discussions* **29** 21
[27] Petek H, Ogawa S 1997 *Prog. Surf. Sci.* **56** 239
[28] Weinelt M 2002 *J. Phys.: Cond. Mat.* **14**, R1099
[29] Harris C B, Ge N H, Lingle R L, McNeill J D and Wong C M 1997 *Ann. Rev. Phys. Chem.* **48** 711
[30] Marinica D C, Ramseyer C, Borisov A G, Teillet-Billy D, Gauyacq J P, Berthold W, Feulner P and Höfer U 2002 *Phys. Rev. Lett.* **89** 046802
[31] Rohleder M, Berthold W, Güdde J and Höfer U 2005 *Phys. Rev. Lett.* **94** 017401
[32] Szymanski P, Garrett-Roe S and Harris C B 2005 *Prog. Surf. Sci.* **78** 1
[33] Bovensiepen U 2005 *Prog. Surf. Sci.* **78** 87
[34] Kirchmann P S, Loukakos P A, Bovensiepen U and Wolf M 2005 *New J. Phys.* **7** 113
[35] The kinetic energy E_{kin} is routinely corrected for the contact potential difference of sample and spectrometer.
[36] Stähler J, Meyer M, Kusmierek D O, Bovensiepen U and Wolf M 2007 *in preparation*